Single-Molecule Studies

International Edition: DOI: 10.1002/anie.201502938
German Edition: DOI: 10.1002/ange.201502938

Direct Observation of the Reversible Two-State Unfolding and Refolding of an α/β Protein by Single-Molecule Atomic Force Microscopy**

*Chengzhi He, Chunguang Hu, Xiaodong Hu, Xiaotang Hu, Adam Xiao, Thomas T. Perkins, and Hongbin Li**

Abstract: *Directly observing protein folding in real time using atomic force microscopy (AFM) is challenging. Here the use of AFM to directly monitor the folding of an α/β protein, NuG2, by using low-drift AFM cantilevers is demonstrated. At slow pulling speeds ($< 50\,nm\,s^{-1}$), the refolding of NuG2 can be clearly observed. Lowering the pulling speed reduces the difference between the unfolding and refolding forces, bringing the non-equilibrium unfolding–refolding reactions towards equilibrium. At very low pulling speeds (ca. $2\,nm\,s^{-1}$), unfolding and refolding were observed to occur in near equilibrium. Based on the Crooks fluctuation theorem, we then measured the equilibrium free energy change between folded and unfolded states of NuG2. The improved long-term stability of AFM achieved using gold-free cantilevers allows folding–unfolding reactions of α/β proteins to be directly monitored near equilibrium, opening the avenue towards probing the folding reactions of other mechanically important α/β and all-β elastomeric proteins.*

Protein folding and unfolding is a fundamental event in life, and of vital importance for essentially every single biological process. Understanding protein (un)folding and misfolding mechanisms remains a critically important task in life sciences.[1,2] Improvements in experimental and computational methods continue to cast new insights into this important problem.[3–12] In this regard, AFM-based single molecule force spectroscopy (SMFS) has become a powerful method for investigating protein folding–unfolding dynamics and mechanisms at the single-molecule level, providing new insights that are otherwise impossible to obtain using traditional methods.[4,8,9,11,13–17] The high spatial resolution and fast dynamic response of AFM make it especially appealing for investigating protein dynamics. However, the relatively poor long-term stability of AFM in force[18] makes it challenging to monitor protein folding–unfolding in real time. Although the development of lock-in detection made it possible to observe protein folding,[19] force drift remains the limiting factor for using AFM in protein folding studies.[20–22] Recent progress has led to significant improvements in the long-term stability of AFM, allowing for the folding of small proteins to be directly observed in real time and the full characterization of the folding–unfolding energy landscape.[5,19,22–26] In such experiments, protein folding–unfolding at low stretching forces occur under conditions close to equilibrium, giving distinct (un)folding events accompanied with protein shortening (or lengthening). However, reported direct observations of real-time protein folding using AFM are limited to all-α proteins, such as ankyrin[5,25] and calmodulin.[22–24] These proteins are mechanically labile and unfold at low forces, allowing protein folding and unfolding to occur near equilibrium. However, the direct, real-time observation of the folding of α/β or all-β proteins, which involves the formation of long-range interactions in reaching their native structures, remains challenging and thus underexplored. Thus, SMFS studies of the folding–unfolding of these proteins remain limited to non-equilibrium unfolding reactions, where information about their folding energy landscape remains inaccessible. By leveraging recent improvements in the long-term force stability of AFM by eliminating cantilever drift caused by its metal coating,[21] we directly observed the folding–unfolding of a small α/β protein NuG2 in real time under near-equilibrium conditions. These experiments also enabled us to obtain the first equilibrium free energy information on the folding–unfolding transition of NuG2 from single-molecule AFM experiments.

To examine the feasibility of observing real-rime folding of α/β or all-β proteins, we chose the fast folding α/β protein NuG2 as a model system. NuG2 is a computationally designed variant of the protein GB1, and assumes a characteristic β-grasp fold in which an α-helix packs against a four-stranded β-sheet.[3,27] In our previous single-molecule AFM work, we constructed the polyprotein $(NuG2)_8$, which contains eight identical tandem repeats of NuG2.[28] Owing to the poor long-

[*] C. He, A. Xiao, Prof. Dr. H. Li
Department of Chemistry, University of British Columbia
2036 Main Mall, Vancouver, BC V6T 1Z1 (Canada)
E-mail: Hongbin@chem.ubc.ca
Prof. Dr. C. Hu, Prof. Dr. X. Hu, Prof. Dr. X. Hu, Prof. Dr. H. Li
State Key Laboratory of Precision Measurements Technology and Instruments, School of Precision Instrument and Optoelectronics Engineering, Tianjin University
Tianjin, 300072 (China)
Prof. Dr. T. T. Perkins
JILA, NIST and University of Colorado Boulder
Dept. of Molecular, Cellular, and Developmental Biology
University of Colorado, 440 UCB Boulder, CO 80309 (USA)

[**] This work is supported by the Natural Sciences and Engineering Research Council of Canada, Canada Chairs Program and Tianjin University. H.L. acknowledges the support of a JILA Visiting Fellowship. T.T.P. is a staff member for the Quantum Physics Division of NIST. Mention of commercial products is for information only; it does not imply NIST recommendation or endorsement.

Supporting information for this article is available on the WWW under http://dx.doi.org/10.1002/anie.201502938.

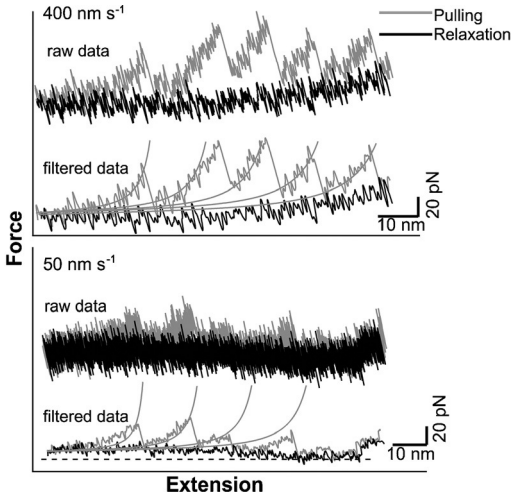

Figure 1. Force–extension (F-E) curves measured using conventional gold-coated Si_3N_4 cantilevers. The sampling frequency for raw data is 10 kHz and the filtered data are low-pass filtered with a corner frequency of 500 Hz. Thin lines are worm-like chain (WLC) fits. The force drift is evident in the bottom curves, as indicated by the dotted line and the deviation of the WLC fits from the data.

term stability of force measurements arising from the cantilever drift, our previous studies on $(NuG2)_8$ were limited to force-induced unfolding reactions under non-equilibrium conditions.[28] In such experiments, the pulling speed had to be greater than 50 nm s^{-1}, as the force drift from the cantilever would overwhelm the experimental signal if the pulling speed were less than 50 nm s^{-1}. Figure 1 shows typical stretching and relaxation force–extension (F-E) curves of $(NuG2)_8$ obtained using a standard gold-coated Si_3N_4 cantilever (MLCT with a spring constant $k \approx 40$ pN nm^{-1}). Stretching $(NuG2)_8$ resulted in F-E curves with a characteristic sawtooth-pattern appearance, where each sawtooth peak corresponds to the mechanical unfolding of one of the NuG2 domains in the polyprotein chain being stretched. Fitting the unfolding events of NuG2 using the worm-like-chain (WLC) model of polymer elasticity[29] measures a contour length increment (ΔL_c) of NuG2 of 18 nm upon complete unfolding, in good agreement with our previous measurements as well as the value calculated from the structure of NuG2.[28] In contrast to the sawtooth-like F-E curves observed when NuG2 unfolds, refolding of this protein results in largely featureless spectra, with no clear refolding events at both pulling speeds of 400 nm s^{-1} and 50 nm s^{-1}. Large hysteresis exists between unfolding and refolding traces, demonstrating that the unfolding of NuG2 at these pulling speeds occurs under a non-equilibrium condition. Furthermore, drift in the force signal is evident in the F-E curves at 50 nm s^{-1} (Figure 1, bottom).

To improve the long-term stability of AFM force measurements, Churnside et al. developed a simple yet effective method: removing the gold coating from the cantilevers by wet etching can significantly reduce the force drift of the cantilever (Biolever, $k = 6$ pN nm^{-1}), and greatly improve the long-term stability of AFM without affecting the signal-to-noise ratio of F-E measurements.[21] Using this method, we prepared uncoated cantilevers and used them to measure the F-E curves of NuG2 at low pulling speeds. Indeed, we found that using uncoated cantilevers significantly improves the long-term stability of F-E measurements, and F-E experiments at pulling speed as low as 1 nm s^{-1} become possible in a state-of-the-art commercial AFM (Asylum Cypher). Figure 2 A shows stretching and relaxation curves of NuG2 at a pulling speed of 400, 50, and 2 nm s^{-1}, respectively. In these spectra at 50 nm s^{-1} and 2 nm s^{-1}, features slightly greater than the noise are clearly visible. After filtering the data to 500 Hz using a low-pass filter, sawtooth-like F-E curves are evident in both stretching and relaxation traces. This pattern clearly indicates that NuG2 displays refolding events during relax-

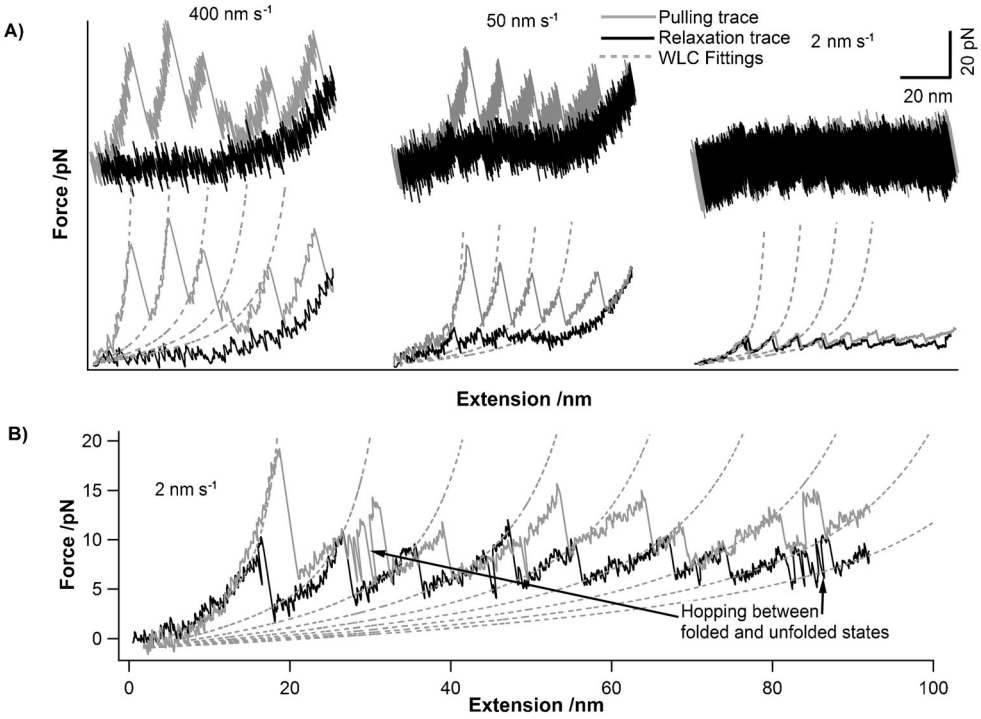

Figure 2. Improved SMFS experiments using uncoated cantilevers. A) Comparison of pulling (solid gray) and relaxation (solid black) curves of $(NuG2)_8$ at different pulling speeds. Raw and filtered F-E traces are shown on the top and bottom, respectively. Dashed lines correspond to WLC fits to the data. The force peaks in the pulling traces and force valleys in the relaxation traces correspond to unfolding and folding events, respectively. B) Typical low-pass-filtered pulling and relaxation traces of $(NuG2)_8$ at a pulling speed of 2 nm s^{-1}. Occurrences when the protein hops between folded and unfolded states are shown by arrows.

ation, which are manifested as the shortening of the taut polypeptide chain and a corresponding increase in force. At these pulling speeds (50 nm s^{-1} and 2 nm s^{-1}), the hysteresis between unfolding and refolding traces, which represents the energy dissipation under the non-equilibrium conditions, becomes significantly smaller than that at 400 nm s^{-1}. Moreover, when the pulling speed is 20 nm s^{-1} or less, we observed rapid hopping events between adjacent WLC F-E curves in both stretching and relaxation (Figure 2B). During this hopping, the NuG2 transitions between two states, indicating that unfolding–refolding transitions are occurring at similar rates and thus approaching equilibrium. Such a phenomenon has been observed in calmodulin[22,24] and ankyrin.[5,25,26]

We carried out stretching–relaxation experiments at pulling speeds from 2 to 2000 nm s^{-1}, and measured the pulling speed dependence of the unfolding and refolding force, respectively (Figure 3). As expected, the unfolding force of NuG2 decreases as pulling speed decreases, while the refolding force increases with decreasing relaxation speed (Figure 3B). At the lowest pulling speed, the unfolding and refolding forces of NuG2 are becoming closer to each other. If the pulling speed were low enough, unfolding–refolding transitions would occur near equilibrium and on average, no hysteresis would exist between stretching and relaxation traces. The difference between unfolding and refolding forces would reach a minimum value, which is caused by the extension or shortening of the polypeptide chain upon (un)folding in F-E experiments. Thus, under very low pulling speeds, the unfolding and folding forces would approach their asymptotic values, giving rise to different pulling speed dependency of the unfolding force at low pulling speeds than that at faster speeds (non-equilibrium regime). Our data clearly displays such a trend (Figure 3B): the unfolding force increases rapidly with increasing pulling speed at pulling speeds higher than 10 nm s^{-1}; while unfolding force becomes less sensitive to pulling speed at lower pulling speed (<10 nm s^{-1}). Such a change of pulling speed dependency of unfolding forces is clearly different from those resulting from two different energy barriers in the unfolding/unbinding energy landscape or the shift of the unfolding pathway.[30,31]

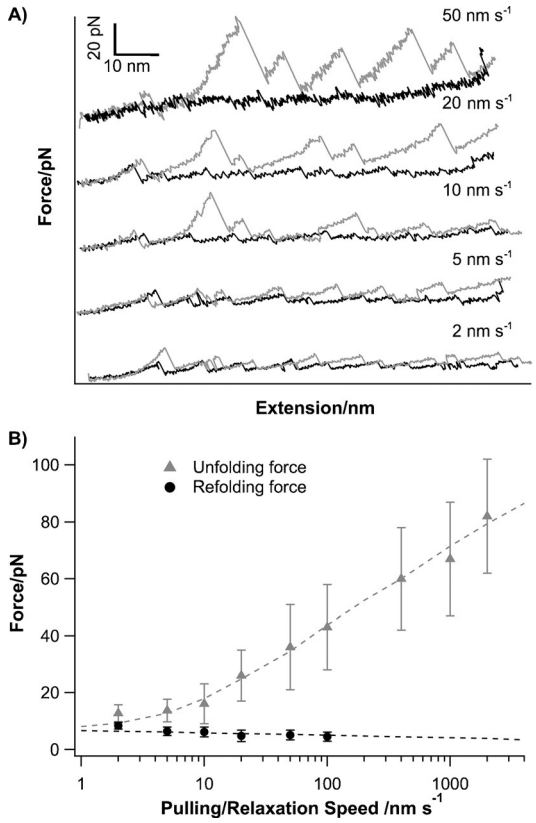

Figure 3. A) F-E curves of $(NuG2)_8$ polyproteins obtained at different pulling speeds. Pulling curves and relaxation curves are in gray and black, respectively. B) Pulling/relaxation speed dependency of the unfolding–refolding force of NuG2. Dashed lines are Monte Carlo simulation results.

To estimate key parameters characterizing the unfolding–folding energy landscape of NuG2, Monte Carlo simulations that represent the exact experimental conditions were performed and the resultant data was used to "fit" the pulling speed dependency of unfolding/refolding forces.[30,32–34] Representative simulated F-E curves are shown in the Supporting Information, Figure S1. We found that an unfolding rate constant α_0 of 0.04 s^{-1} and the distance to the transition state Δx_u of 0.42 nm well describe the experimental data (Supporting Information), indicating that NuG2s mechanical unfolding transition state is very close to its native state. In contrast, a folding rate constant at zero force β_0 of 10000 s^{-1} and a folding distance Δx_f of 5 nm were found to be sufficient to describe the experimental data. This fast-folding makes it possible to observe the hopping of NuG2 between folded and unfolded states in real-time. Analysis of these rates using $\Delta G^0 = k_B T \ln(\beta_0/\alpha_0)$ yields a free energy difference of about 12.4 k_BT at $F = 0$ pN between the native and unfolded states.

It is of note that Δx_u estimated here (0.42 nm) is slightly larger than that reported in our previous force-clamp spectroscopy study (0.25 nm), where stiffer cantilevers ($k =$ 40 pN nm^{-1}) were used than those in the current study (6 pN nm^{-1}). Previous SMFS studies on calmodulin also showed similar difference.[22,33] The reason underlying this difference is unclear and deserves a systematic investigation.

Unfolding–refolding transitions of NuG2 observed in our AFM experiments were non-equilibrium in nature, and thus associated with hysteresis. Using fluctuation theorems, one can relate the work along non-equilibrium trajectories to thermodynamic free energy differences between states; these methods have been previously used in optical tweezers studies to obtain information on the folding energy landscape of proteins and nucleic acids.[35–38] Here, we examine the feasibility of using Crooks fluctuation theorem (CFT)[35,36] to determine the equilibrium free energy difference ΔG^0 between folded and unfolded states from such non-equilibrium force vs. distance curves in AFM experiments. CFT allows the amount of hysteresis associated with irreversible work done to unfold and refold a protein to be quantified, and relate this irreversible work to ΔG^0 through the following equation:

$$\frac{P_U(w)}{P_R(w)} = \exp\left(\frac{w-\Delta G^0}{k_B T}\right)$$

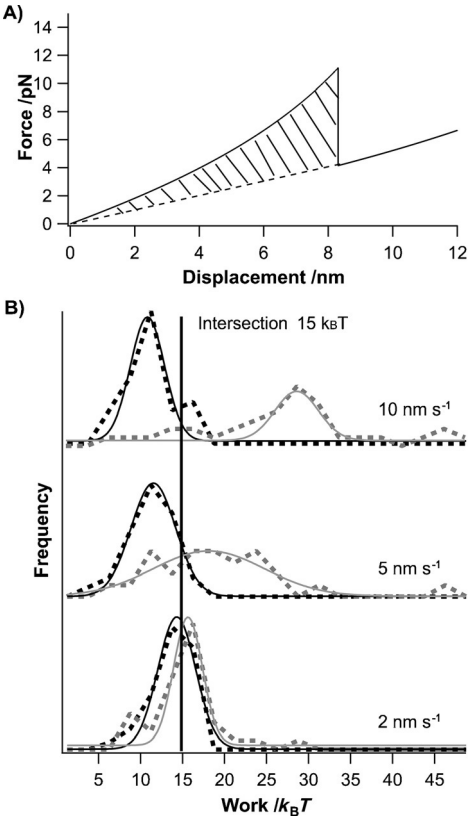

Figure 4. Crooks fluctuation theorem analysis of NuG2 unfolding–folding. A) The data analysis process. The area enclosed by the experimental force peak (solid curve) and WLC fit (dashed curve) is shaded. B) Normalized histograms (dashed lines) represent unfolding work (gray) and refolding work (black). Solid lines are Gaussian fits to the data. The intersection of unfolding and refolding work (ca. 15 $k_B T$) is measured from the Gaussian fits.

where $P_U(w)$ and $P_R(w)$ correspond to the work distribution associated with unfolding and refolding of the protein. As shown in Figure 4, the intersection between $P_U(w)$ and $P_R(w)$ yields the equilibrium free energy difference ΔG^0 of 15 $k_B T$ for NuG2, which is close to ΔG^0 obtained from Monte Carlo simulations (Supporting Information). Thus, CFT can be used in AFM-based SMFS experiments that employ much stiffer probes (6 pN nm^{-1}) to determine the equilibrium free energy than those used in optical-trapping experiments (0.2 pN nm^{-1}), given sufficient instrumental stability.

In summary, using single-molecule AFM with improved long-term stability and force resolution, we directly observed the real-time folding and unfolding of a small α/β protein NuG2 near equilibrium, allowing us to directly determine the equilibrium free energy difference between its folded and unfolded states from single-molecule experiments for the first time. Our studies expand the range of proteins that can be examined using AFM under conditions that approach equilibrium, which may allow for the examination of elastomeric proteins, such as the giant muscle protein titin and extracellular matrix protein fibronectin, at forces that are physiologically relevant. Such experiments would greatly support further understanding of the elastic behavior of these elastomeric proteins in their biological settings.

Keywords: atomic force microscopy · fluctuation theorem · force spectroscopy · protein folding · single-molecule studies

How to cite: *Angew. Chem. Int. Ed.* **2015**, *54*, 9921–9925
Angew. Chem. **2015**, *127*, 10059–10063

[1] C. M. Dobson, A. Sali, M. Karplus, *Angew. Chem. Int. Ed.* **1998**, *37*, 868–893; *Angew. Chem.* **1998**, *110*, 908–935.
[2] I. Luque, S. A. Leavitt, E. Freire, *Annu. Rev. Biophys. Biomol. Struct.* **2002**, *31*, 235–256.
[3] S. Nauli, B. Kuhlman, D. Baker, *Nat. Struct. Biol.* **2001**, *8*, 602–605.
[4] A. Borgia, P. M. Williams, J. Clarke, *Annu. Rev. Biochem.* **2008**, *77*, 101–125.
[5] W. Lee, X. C. Zeng, H. X. Zhou, V. Bennett, W. T. Yang, P. E. Marszalek, *J. Biol. Chem.* **2010**, *285*, 38167–38172.
[6] K. Lindorff-Larsen, S. Piana, R. O. Dror, D. E. Shaw, *Science* **2011**, *334*, 517–520.
[7] D. E. Shaw, P. Maragakis, K. Lindorff-Larsen, S. Piana, R. O. Dror, M. P. Eastwood, J. A. Bank, J. M. Jumper, J. K. Salmon, Y. Shan, W. Wriggers, *Science* **2010**, *330*, 341–346.
[8] X. W. Zhuang, M. Rief, *Curr. Opin. Struct. Biol.* **2003**, *13*, 88–97.
[9] G. Žoldák, M. Rief, *Curr. Opin. Struct. Biol.* **2013**, *23*, 48–57.
[10] C. Cecconi, E. A. Shank, C. Bustamante, S. Marqusee, *Science* **2005**, *309*, 2057–2060.
[11] J. M. Fernandez, H. B. Li, *Science* **2004**, *303*, 1674–1678.
[12] B. Schuler, H. Hofmann, *Curr. Opin. Struct. Biol.* **2013**, *23*, 36–47.
[13] Y. Javadi, J. M. Fernandez, R. Perez-Jimenez, *Physiology* **2013**, *28*, 9–17.
[14] P. E. Marszalek, Y. F. Dufrene, *Chem. Soc. Rev.* **2012**, *41*, 3523–3534.
[15] X. Hu, H. Li, *FEBS Lett.* **2014**, *588*, 3613–3620.
[16] N. Crampton, D. J. Brockwell, *Curr. Opin. Struct. Biol.* **2010**, *20*, 508–517.
[17] T. Hoffmann, K. M. Tych, M. L. Hughes, D. J. Brockwell, L. Dougan, *Phys. Chem. Chem. Phys.* **2013**, *15*, 15767–15780.
[18] G. M. King, A. R. Carter, A. B. Churnside, L. S. Eberle, T. T. Perkins, *Nano Lett.* **2009**, *9*, 1451–1456.
[19] M. Schlierf, F. Berkemeier, M. Rief, *Biophys. J.* **2007**, *93*, 3989–3998.
[20] A. B. Churnside, T. T. Perkins, *FEBS Lett.* **2014**, *588*, 3621–3630.
[21] A. B. Churnside, R. M. A. Sullan, D. M. Nguyen, S. O. Case, M. S. Bull, G. M. King, T. T. Perkins, *Nano Lett.* **2012**, *12*, 3557–3561.
[22] J. P. Junker, F. Ziegler, M. Rief, *Science* **2009**, *323*, 633–637.
[23] Z. T. Yew, M. Schlierf, M. Rief, E. Paci, *Phys. Rev. E* **2010**, *81*, 031923.
[24] J. P. Junker, M. Rief, *Angew. Chem. Int. Ed.* **2010**, *49*, 3306–3309; *Angew. Chem.* **2010**, *122*, 3378–3381.
[25] W. Lee, X. C. Zeng, K. Rotolo, M. Yang, C. J. Schofield, V. Bennett, W. T. Yang, P. E. Marszalek, *Biophys. J.* **2012**, *102*, 1118–1126.
[26] G. Lee, K. Abdi, Y. Jiang, P. Michaely, V. Bennett, P. E. Marszalek, *Nature* **2006**, *440*, 246–249.
[27] S. Nauli, B. Kuhlman, I. Le Trong, R. E. Stenkamp, D. Teller, D. Baker, *Protein Sci.* **2002**, *11*, 2924–2931.
[28] Y. Cao, R. Kuske, H. B. Li, *Biophys. J.* **2008**, *95*, 782–788.
[29] J. F. Marko, E. D. Siggia, *Macromolecules* **1995**, *28*, 8759–8770.
[30] E. Evans, *Annu. Rev. Biophys. Biomol. Struct.* **2001**, *30*, 105–128.
[31] B. Jagannathan, P. J. Elms, C. Bustamante, S. Marqusee, *Proc. Natl. Acad. Sci. USA* **2012**, *109*, 17820–17825.
[32] G. I. Bell, *Science* **1978**, *200*, 618–627.
[33] J. Stigler, F. Ziegler, A. Gieseke, J. C. M. Gebhardt, M. Rief, *Science* **2011**, *334*, 512–516.

[34] A. F. Oberhauser, P. E. Marszalek, H. P. Erickson, J. M. Fernandez, *Nature* **1998**, *393*, 181 – 185.
[35] G. E. Crooks, *Phys. Rev. E* **1999**, *60*, 2721 – 2726.
[36] D. Collin, F. Ritort, C. Jarzynski, S. B. Smith, I. Tinoco, C. Bustamante, *Nature* **2005**, *437*, 231 – 234.
[37] E. A. Shank, C. Cecconi, J. W. Dill, S. Marqusee, C. Bustamante, *Nature* **2010**, *465*, 637 – 640.
[38] J. C. M. Gebhardt, T. Bornschlogla, M. Rief, *Proc. Natl. Acad. Sci. USA* **2010**, *107*, 2013 – 2018.

Received: March 30, 2015
Revised: May 6, 2015
Published online: July 1, 2015

